Entanglement scaling of excited states
in large one-dimensional many-body localized systems

D. M. Kennes[1] and C. Karrasch[2]

[1]*Institut für Theorie der Statistischen Physik, RWTH Aachen University and*
JARA-Fundamentals of Future Information Technology, 52056 Aachen, Germany and
[2]*Dahlem Center for Complex Quantum Systems and Fachbereich Physik,*
Freie Universität Berlin, 14195 Berlin, Germany

We study the properties of excited states in one-dimensional many-body localized (MBL) systems using a matrix product state algorithm. First, the method is tested for a large disordered non-interacting system, where for comparison we compute a quasi-exact reference solution via a Monte Carlo sampling of the single-particle levels. Thereafter, we present extensive data obtained for large interacting systems of $L \sim 100$ sites and large bond dimensions $\chi \sim 1300$, which allows us to quantitatively analyze the scaling behavior of the entanglement S in the system. The MBL phase is characterized by an area law with logarithmic corrections, $S(L)/L \sim \log(L)/L$. We check the validity of the eigenstate thermalization hypothesis. Our results are consistent with the existence of a mobility edge.

I. INTRODUCTION

Disorder such as impurities or vacancies is present in every physical system. Our basic understanding of its effects goes back to Anderson [1]: Roughly speaking, the ratio between the electron wavelength and the mean free path determines whether states are extended or localized and hence whether the system is a metal or an insulator. In one or two spatial dimensions, an arbitrarily small amount of disorder will localize any eigenstate in the spectrum, but in 3d a so-called mobility edge can exist which separates localized states at the lower end of the spectrum from extended states at high energies. The transition, which can, e.g., be triggered by varying the disorder strength, is the so-called Anderson transition. Three distinct properties of the localized phase are that a) the DC conductivity σ vanishes in the thermodynamic limit at any finite temperature (if all single-particle states are localized, i.e. in absence of a mobility edge), b) the system does not thermalize, but information about an initial state is preserved in local observables during a unitary time evolution, and c) the entanglement entropy is not extensive but features an area law. Reviews of these single-particle localization physics can be found in Refs. [2–4].

Anderson localization is formulated for free particles; one might wonder whether interactions delocalize every state, render the conductivity finite and lead to thermalization. In a seminal work, however, Basko, Aleiner, and Altshuler suggested that the localized phase can exist even in presence of interactions and that a finite temperature phase transition can exist between phases with $\sigma = 0$ and $\sigma > 0$ [5]. This phase transition is not a thermodynamic (equilibrium) transition but a dynamical quantum phase transition which occurs on the level of the many-body eigenstates and defies standard Mermin-Wagner arguments.

In contrast to localization in a non-interacting system, the world of many-body localization (MBL; see Ref. [6]

for a recent review) is still comparably young. Basko, Aleiner and Altshuler's idea was based on perturbative arguments whose range of validity for a given microscopic model is a priori unclear. For one-dimensional lattice systems, the stability of localized states towards adding interactions – i.e., the existence of the MBL phase – has subsequently been established fairly convincingly by a number of numerical [7–14] and analytical [15–17] studies. Moreover, there is now solid evidence that a transition into a delocalized phase occurs if the ratio between the interaction and the disorder strength is increased [10, 12–14]. The MBL phase was characterized via level statistics [7, 10], entanglement measures [11, 12, 18], or thermalization behavior [10, 19]. Some experimentally-accessible observables were computed such as transport properties [20–27] or spectral features in presence of a bath [28, 29]. MBL physics was observed experimentally in a cold atom setup [30, 31].

However, even in 1d there is a variety of open questions. First, most of the above-mentioned studies were based on an exact diagonalization of small systems, and since it is unclear how to properly perform a finite-size scaling, very little is known about the nature of the dynamical phase transition between the MBL and the metallic phases (e.g., its universality class). Second, the issue of a many-body mobility edge in 1d (its existence and how it depends on the model parameters) is still debated [32], and so is the ensuing question of a quantitative description of the MBL transition as a function of the temperature.

One route to deepen our understanding of many-body localization physics is to approach the problem using different methods which have their own strengths and shortcomings. In particular, it would be highly desirable to study systems which are larger than those accessible by exact diagonalization. In one dimension, the density matrix renormalization group (DMRG) allows to elegantly compute ground states (or finite-entanglement approximations thereof) as well as those excited states which cor-

respond to ground states in different symmetry sectors. In order to describe MBL physics, however, one needs access to generic excited states. Even though many-body localized states feature an entanglement area law and can thus in principle be expressed efficiently as a matrix product state (MPS) [33], no algorithm (see below for comments on two recent preprints) exits to determine this MPS representation in practice.

It is our goal to introduce a very simple MPS-based framework to calculate excited states of MBL systems. We first test the method for the non-interacting case, where we construct eigenstates at a given energy via a Monte Carlo sampling of the known single-particle levels. We then present extensive data for large systems of $L \sim 100$ sites obtained for large bond dimensions of $\chi \sim 1300$. This allows us to quantitatively analyze the scaling of the entanglement entropy. We also verify the violation of the eigenstate thermalization hypothesis. Indications of a crossover into the metallic phase and the existence of a mobility edge are presented.

Shortly before the completion of our work, we became aware of two preprints [34, 35] which present similar ideas to access excited states of MBL systems via DMRG algorithms (another method to compute features of the entire spectrum rather than individual states was introduced in preprint [36]). We complement these studies in the following way: Our data was obtained over the course of 6 months using large-scale numerics (350.000 core hours); this allows us to access systems which are larger than those investigated in Refs. [34, 35], which in turn yields new quantitative insights about the precise scaling of the entanglement in the MBL phase. Moreover, we re-examine the question of a mobility edge from an entanglement perspective.

II. MODEL AND METHOD

A. Model

We consider one-dimensional spinless interacting fermions living on a lattice of size L, or equivalently, a XXZ spin chain:

$$H = \sum_{l=1}^{L} \left(\frac{1}{2} S_l^+ S_{l+1}^- + \text{h.c.} + \Delta S_l^z S_{l+1}^z + V_l S_l^z \right), \quad (1)$$

where $S^{x,y,z}$ are spin-1/2 operators, and $S^{\pm} = S^x \pm iS^y$. The on-site potentials are drawn from a uniform random distribution:

$$V_l \in [-\eta, \eta]. \quad (2)$$

Prior numerics suggest that a transition between a fully many-body localized and a metallic phase occurs around $\eta \sim 3.5$ (see, e.g., Ref. [13] for an exact diagonalization study of up to $L = 22$ sites).
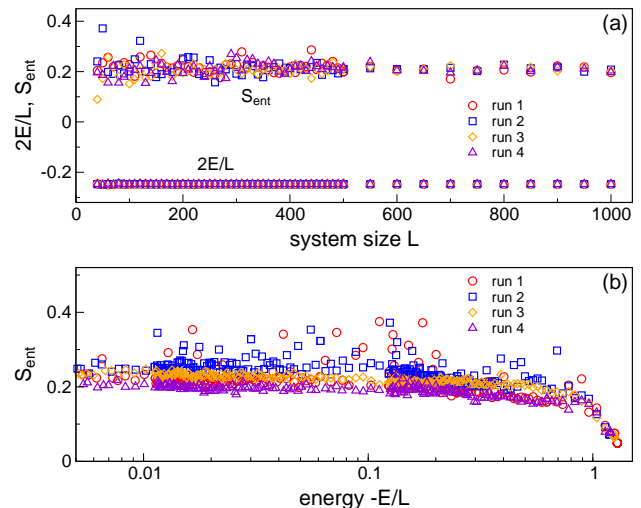

FIG. 1. (Color online) Proof-of-principle application of the excited-state DMRG algorithm to a non-interacting system ($\Delta = 0$) with disorder $\eta = 5$. (a) System-size dependence of the entanglement entropy in highly-excited states with an energy density $E/L \approx -0.125$; the area law holds. Four different disorder realizations are shown at each L [$4 *$ (number of L-points) realizations in total]. The data was obtained using a constant mixing λ. (b) The same but for a constant system size $L = 200$ and four different disorder configurations. The entire energy spectrum was scanned by heuristically varying λ.

B. DMRG for excited states

The density matrix renormalization group [37, 38] provides an algorithm to variationally compute the ground state within the class of matrix product states. The matrix (bond) dimension χ encodes the amount of entanglement S in the system. If the problem at hand features an area law, S is non-extensive, and the ground state can thus be represented exactly by a MPS with a finite χ even in the thermodynamic limit. More generally, one can think of the DMRG as a tool to determine finite-entanglement approximations.

Generalizations of the DMRG algorithm allow to compute (approximations to) a few low-lying excited states as well as those excited states which correspond to ground states in a different symmetry sector [37]. However, a practical way to extract arbitrary states in the spectrum does not exist even if it is known that they can in principle be expressed efficiently by a MPS due to their finite entanglement; this is exactly the case in localized systems. Moreover, many-body localization cannot be understood by only considering ground states, and developing a tool to determine the MPS representation of lowly-entangled excited states is thus desirable.

We introduce a simple scheme to calculate finite-entanglement approximations of generic excited states in localized systems. Its basic idea is to consider a set of auxiliary operators $f_\lambda(H)$ whose ground states corre-

spond to excited states of the original Hamiltonian H. This implies that any existing DMRG code can be used straightforwardly for the calculation. The only a priori requirements is that $f_\lambda(H)$ can be written as a matrix product operator of low dimension. Here, we employ (we will comment on potential pitfalls associated with this choice below)

$$f_\lambda(H) = \lambda H + (1-\lambda)H^2\,, \tag{3}$$

which for the Hamiltonian of Eq. (1) can be written as a MPO of dimension 9:

$$W^{[l]} = \begin{pmatrix} M_1^l & 0 \\ M_2^l & M_3^l \end{pmatrix}\,, \tag{4}$$

where for $l \neq 1, L$:

$$M_1^l = \begin{pmatrix} I & 0 & \dots \\ \frac{S^-}{2} & 0 & \dots \\ \frac{S^+}{2} & 0 & \dots \\ S^z & 0 & \dots \end{pmatrix}\,, \quad M_3^l = \begin{pmatrix} \vdots & \vdots & \vdots & \vdots \\ 0 & 0 & 0 & 0 \\ S^+ & S^- & S^z & I \end{pmatrix}\,, \tag{5}$$

and

$$M_2^l = \begin{pmatrix} 2V_l(1-\lambda)\Delta & 2(1-\lambda)S^+ & 2(1-\lambda)S^- & 2\Delta(1-\lambda)S^z & I \\ 0 & \frac{1-\lambda}{2}I & 0 & 0 & \frac{S^-}{2} \\ 0 & 0 & \frac{1-\lambda}{2}I & 0 & \frac{S^+}{2} \\ 0 & 0 & 0 & \frac{\Delta^2(1-\lambda)}{2}I & \Delta S^z \\ \lambda V_l + \frac{V_{l-1}+V_{l+1}}{2}\Delta(1-\lambda)S^z & \left[\lambda - \frac{\Delta(1-\lambda)}{2}\right]S^+ & \left[\lambda - \frac{\Delta(1-\lambda)}{2}\right]S^- & \left[\Delta\lambda - \frac{1-\lambda}{2}\right]S^z & V_l(1-\lambda)S^z \end{pmatrix}\,. \tag{6}$$

We determine the ground state of $f_\lambda(H)$ using a standard two-site DMRG algorithm [37]. The discarded weight is fixed (we have checked that lowering it further does not change our results); hence, the bond dimension χ increases during the DMRG sweeps. Our calculations are carried out using even system sizes L and in a fixed symmetry sector $\langle \sum_{l=1}^L S_l^z \rangle = 0$. Convergence is checked via the variance of the energy; we allow for a comparably large value $\mathrm{var}(H) \sim 10^{-6} \gg e^{-L}$. Hence, we can a priori only expect to obtain *superpositions* of nearby eigenstates. More comments on this issue will be given below.

In order to gain some further understanding of the capabilities as well as the potential pitfalls of this algorithm, it is instructive to consider the case of free fermions in absence of disorder ($\Delta = \eta = 0$). The spectrum of H is then simply characterized by the single-particle states $\epsilon_k = -\cos(k)$, and it is intuitively clear that by varying λ one can in principle access excited states at arbitrary energies: While $\lambda = 0$ yields the ground state of H, the spectrum of $f_{\lambda=1}(H) = H^2$ is governed by $\epsilon_k^2 = \cos(k)^2$, and its ground state corresponds to a zero-energy (mid-spectrum) state of H. However, it is also intuitively clear that this state is *special* in the sense that it is always symmetry with respect to $k = \pi/2$ – by construction, our algorithm lacks the capability to describe other (asymmetric) zero-energy states. While this specific issue only occurs at $\lambda = 1$, it gives rise to the general question of whether or not the states targeted by our algorithm are generic. We will come back to this below.

Moreover, the spacing between individual eigenstates generally decreases *exponentially* with the system size. Hence, for large $L \sim 100$ (which we want to access in

this work), it is a priori unclear whether our approach will produce pure eigenstates or superpositions of nearby eigenstates. In the latter case, it is not obvious whether or not one can reasonably study physical questions (e.g., the scaling behavior of the entanglement or the violation of the eigenstate thermalization hypothesis) from a superposition. In Ref. [34], it is nicely explained how to resolve individual eigenstates in localized systems despite the exponentially small level spacing. For our purposes, however, it turns out that employing this (more elaborate) algorithm is not necessary.
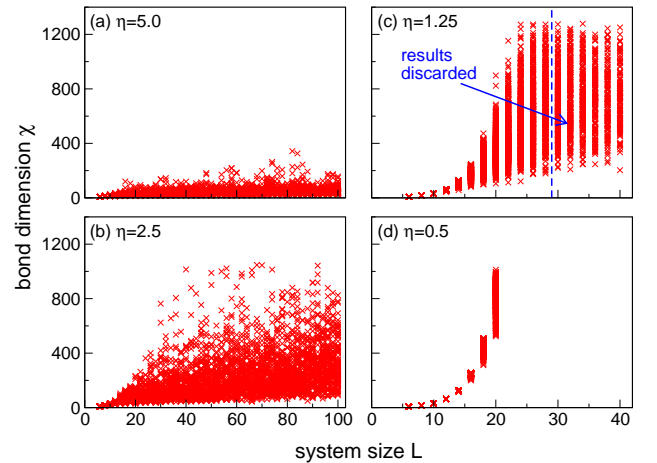

FIG. 2. (Color online) Scatter plot of the bond dimensions χ occurring in the DMRG calculation of a highly-excited state with energy $E/L = -0.125$ in a non-interacting system ($\Delta = 0$) of size L. (a–d) show various disorder strengths η; the total number of configurations in each panel is $O(5000)$.
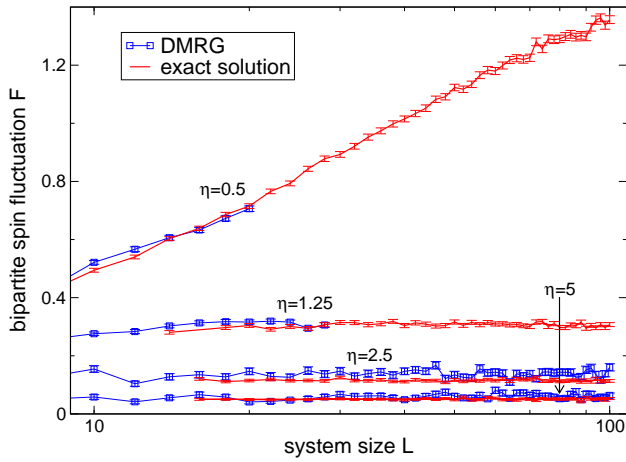
FIG. 3. (Color online) Scaling of the bipartite spin fluctuations $F(L)$ corresponding to the data sets shown in Fig. 2. For comparison, an analytic reference solution is constructed from the exact diagonalization of the non-interacting Hamiltonian combined with a Monte Carlo sampling of the single-particle levels to determine excited states with $E/L = -0.125$. The error bars are defined via the standard deviation of F.

FIG. 4. (Color online) The same as in Fig. 2 but for an isotropic XXZ chain ($\Delta = 1$), fixed disorder $\eta = 2.5$ but various energies E/L. Each panel shows data for $O(5000)$ configurations.

To summarize, the following potential problems/questions need to be addressed: a) What can one learn if only superpositions of nearby eigenstates are accessible?, b) Are the states/results that one obtains from our simple algorithm generic?, and c) How do we need to choose λ in order to target states at a given energy density?

It turns out that one can answer c) pragmatically – the value of λ can be determined numerically by simple trial-and-error; this is not a bottleneck in the calculation. For all data shown for system sizes of $L > 10$ sites, λ was chosen such that a targeted energy density E/L is reached with a relative accuracy of at most one percent (deviations are larger for $L \leq 10$ where the spectrum is less dense; since such small systems are of little interest, we refrain from further investigations). More details regarding the choice of λ can be found in Sec. III.

One can partially answer a) and b) using physical arguments: One expects that states which are close in energy feature a similar scaling of the entanglement entropy – on the other hand, local observables in the MBL phase should differ vastly between different eigenstates, and if one can observe this violation of the ETH within our approach, one could be pragmatically satisfied. However, a more cautious way to tackle a) and b) is to solve the non-interacting, disordered problem ($\Delta = 0, \eta > 0$) analytically; since this limit is not special for the DMRG, it provides an unbiased frame of reference.

C. Exact solution at $\Delta = 0$

At $\Delta = 0$, the Hamiltonian of Eq. (1) maps to spinless, non-interacting fermions and can thus be solved exactly.
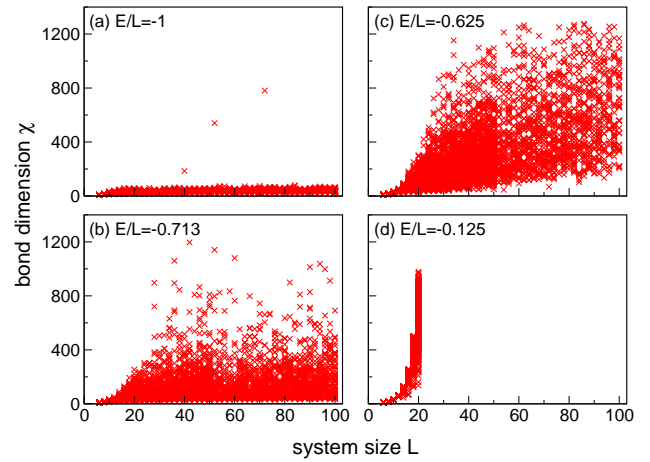
For any given disorder realization, the single-particle energies ϵ_i are simply obtained by diagonalizing a $L \times L$ matrix, and the many-body eigenstates are given by arbitrarily filling up $L/2$ of these levels (which corresponds to zero magnetization in the spin language). In order to obtain an eigenstate at (approximately) a given energy E/L, we need to find the occupation numbers $n_i \in \{0, 1\}$ for which $\sum_i n_i \epsilon_i \approx E$. Since there are $L!/(L/2!)^2$ possibilities to occupy half of all single-particle levels, this combinatorial problem cannot be solved straightforwardly for $L \sim 100$; instead, we propose to employ the following Monte Carlo algorithm:

First, we determine the temperature T of a Fermi distribution such that

$$\sum_{i=1}^{L/2} f_i(T)\epsilon_i = E \,, \ f_i(T) = \frac{1}{\exp(\epsilon_i/T) + 1} \,. \quad (7)$$

Thereafter, we draw L random numbers $s_i \in [0, 1]$ and obtain a 'test configuration' $\{n_i\}$ via

$$n_i = \begin{cases} 0 & s_i \leq f_i(T) \\ 1 & \text{otherwise} \,. \end{cases} \quad (8)$$

The configuration is discarded if $\sum_i n_i \neq L/2$. We repeat this procedure a large number of times and eventually pick the configuration for which $E_0 = \sum_i n_i \epsilon_i$ approximates the given E best. In practice (e.g., for the data shown in Fig. 3), this allows us to find a E_0 that deviates from E by at most one percent within a few seconds.
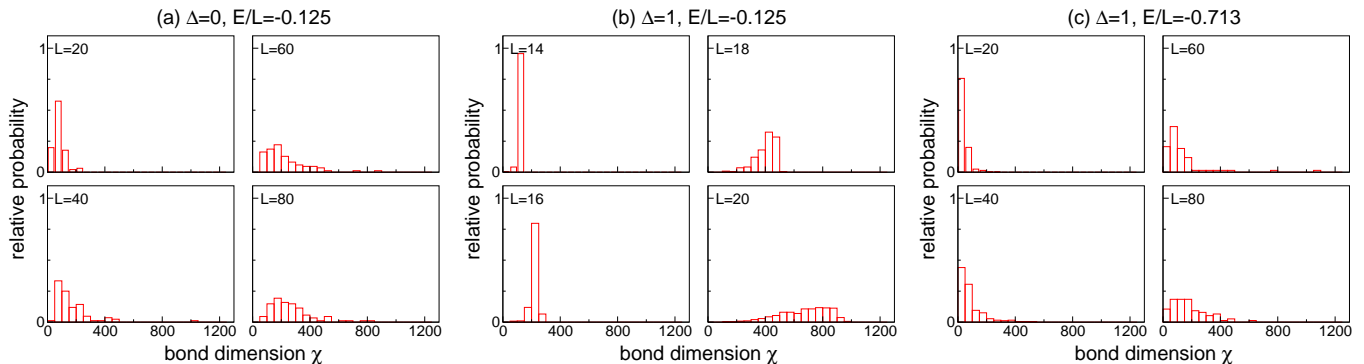
FIG. 5. (Color online) Histogram of the bond dimensions occurring in the DMRG calculation of excited states. The disorder strength is fixed to $\eta = 2.5$, and the system size is increased successively for each parameter set. (a) Non-interacting, localized chain with $E/L = -0.125$ [data corresponding to Fig. 2(b)]. (b) Same energy but in presence of interactions; the system is metallic [data corresponding to Fig. 4(d)]. Note that only small values of L are accessible. (c) At smaller energies, the system becomes many-body localized [data corresponding to Fig. 4(b)].

III. TEST CASE: FREE FERMIONS

A. Raw data

In order to explore the capabilities and limitations of the excited-state DMRG algorithm, we first study the limit $\Delta = 0$ where Eq. (1) maps to non-interacting fermions. In this case, it is known that an arbitrarily small amount of disorder localizes all states in the spectrum. In Figure 1(a), we plot the entanglement entropy S of a highly-excited state with an energy density $E/L \approx -0.125$ for systems of up to $L = 1000$ sites. At each value of L, four different disorder realizations are drawn from a distribution of strength $\eta = 5$. Our results illustrate that the area law $S(L)/L \to 0$ holds, reflective of the fact that this state is localized.

In Fig. 1(b), we demonstrate that the mixing λ can be easily varied such that states at all energies can be accessed (the calculation was carried out for fixed $L = 200$ and four different disorder configurations). For illustrative purposes, the data in Fig. 1(a) was obtained using a *constant* mixing λ, confirming the expectation that at sufficiently large L a given energy density E/L can be targeted using the same λ irrespective of the concrete disorder configuration. This greatly facilitates the numerical determination of λ.

Next, we compute excited states at a fixed energy density $E/L = -0.125$ for a large number of disorder realizations and system sizes. Figure 2 shows a scatter plot of the bond dimensions χ necessary to describe these states. In general, smaller η require larger values of χ, which is reasonable since one expects the correlation length and hence the amount of entanglement to increase with decreasing strength of the disorder. Moreover, Fig. 2 shows the occurrence of rare states with unusually high entanglement (see below).

Only finite bond dimensions are accessible numerically due to the limitation of computational resources. In this

work, we abort each calculation once χ exceeds a value of $\chi = 1300$. In order to reliably compute averaged quantities, we need to ensure that the states dropped in our calculation are only rare states which do not carry any substantial weight. To this end one can, e.g., successively increase the system size and determine histograms of bond dimensions for each L (see Fig. 5 for an example). We eventually discard all data for which substantial weight is shifted above $\chi \sim 1300$ – e.g., at $\eta = 1.25$ and $E/L = -0.125$, averages can only be computed up to $L \sim 28$ [see Fig. 2(c)].

B. Comparison with the exact solution

Finally, we need to address the issues outlined in Sec. II B: Are the excited states determined by our algorithm generic, and is it reasonable to allow for a fairly large energy variance and to study the physics not using exact eigenstates but potentially using a superposition of nearby states? We therefore use the exact solution introduced in Sec. II C as a frame of reference; in particular, we compare the system-size dependence of the bipartite fluctuations of the magnetization,

$$F = \langle (S_A^z)^2 \rangle - \langle S_A^z \rangle^2 , \ S_A^z = \sum_{l=1}^{L/2} S_l^z . \qquad (9)$$

We employ F instead of the entanglement S since it is expected to feature similar scaling behavior [13] but exhibits somewhat smaller fluctuations and is hence better suited for a quantitative comparison (we will present exact data for the scaling of S at $\Delta = 0$ in the context of the discussion in Sec. IV). Results are shown in Fig. 3, indicating that our method can indeed be used to study the generic properties of states at a given energy density.
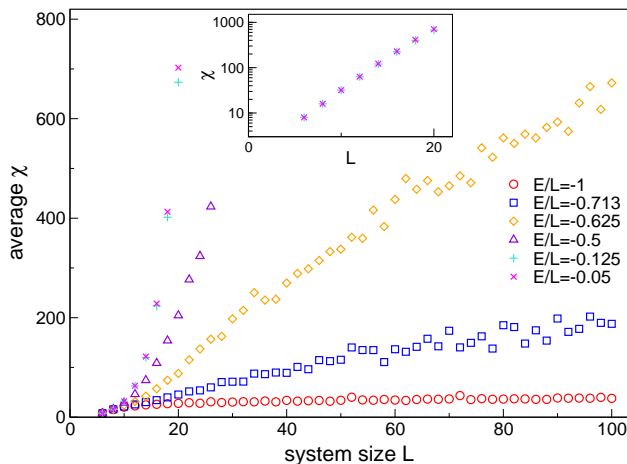
FIG. 6. (Color online) Scaling of the average bond dimension for fixed, intermediate-strength disorder $\eta = 2.5$ and various excited-state energies E/L for an isotropic XXZ chain ($\Delta = 1$). The metallic phase is characterized by $\chi \sim e^L$; the entanglement features a volume law $S(L) \sim L$. In the many-body localized regime, our data suggests $\chi \sim L$ and hence an area-law scaling of the entanglement with sub-leading logarithmic corrections, $S(L) \sim \log(L)$. The results are consistent with the existence of a mobility edge at $\eta = 2.5$.

IV. MANY-BODY LOCALIZED REGIME

A. Raw data

We now use our DMRG algorithm to investigate the many-body localization physics of excited states. As mentioned above, similar studies appeared shortly before the completion of our paper [34, 35]. Our results were obtained using long-term, large-scale numerics for large systems and hence complement and extend the data presented in Refs. [34, 35].

The isotropic XXZ chain ($\Delta = 1$) was recently diagonalized exactly for up to $L = 22$ sites [13], indicating that all states in the spectrum are localized if $\eta \gtrsim 4$. The data for weaker disorder is consistent with a coexistence of metallic states at high energies and localized states at the lower end of the spectrum. However, it was later conjectured that these results are plagued by severe finite-size effects, and the existence of a mobility edge was disputed [32].

Fig. 4 shows a scatter plot of the bond dimensions occurring during the calculation of excited states at $\eta = 2.5$ for various energy densities. As a reminder, we employ a two-site DMRG algorithm using a fixed discarded weight; hence, the bond dimension automatically increases to encode the amount of entanglement present in the targeted state. One can see that while the vast majority of states – each panel shows $O(5000)$ configurations in total – exhibits a bond dimension centered around a certain window, rare states with high entanglement exist at each η and E. They can be identified as Floquet eigenstates and

occur with an exponentially small probability [11, 39–41].

As mentioned above, it is instructive to recast the data shown in Figs. 2 and 4 in terms of histograms in order to illustrate that representative averages can be extracted from our data. For reasons of completeness, we show such histograms in Fig. 5. Panel (a) contains data for $\Delta = 0$ where all states are localized. If the interaction is switched on [panel (b)], the entanglement of states at the same energy increases dramatically (note the different L-scale). Upon lowering the energy, however, χ again grows more slowly. We will now demonstrate that our data is consistent with the states in Fig. 5(b) being metallic while those in Fig. 5(c) are many-body localized.

Finally, a comment about the energy scale associated with the parameters of Fig. 4 is in order. For each individual disorder configuration, the lower and upper edges of the spectrum can be determined using ground state DMRG for $\pm H$. While states with $E/L = -0.125$ correspond to high-energy states near the center of the spectrum, those with $E/L = -1$ are of much lower energy on a scale set by the total bandwidth but still significantly away from the ground state energy (which is located at $E/L \approx -1.5$) and still belong to a dense part of the spectrum with exponentially small level spacings.

B. Scaling of the entanglement; mobility edge

In Fig. 6, we show how the average bond dimension at $\Delta = 1$ and intermediate disorder $\eta = 2.5$ scales with the system size. At low energy densities (large $-E/L$), χ grows linearly with L, implying that the entanglement in the many-body localized phase exhibits an area law with
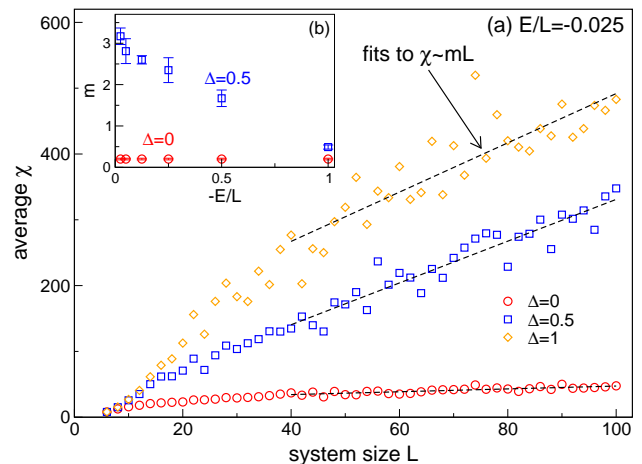

FIG. 7. (Color online) (a) The same as in Fig. 6 but for a large value $\eta = 5$ deep in the MBL phase, fixed $E/L = -0.025$, and various interactions Δ. The system is localized, and the average bond dimension scales linearly with the system size, $\chi \sim mL$. (b) Energy-dependence of the prefactor m for $\Delta = 0$ and $\Delta = 0.5$. We extracted m from linear fits for $L > 40$.
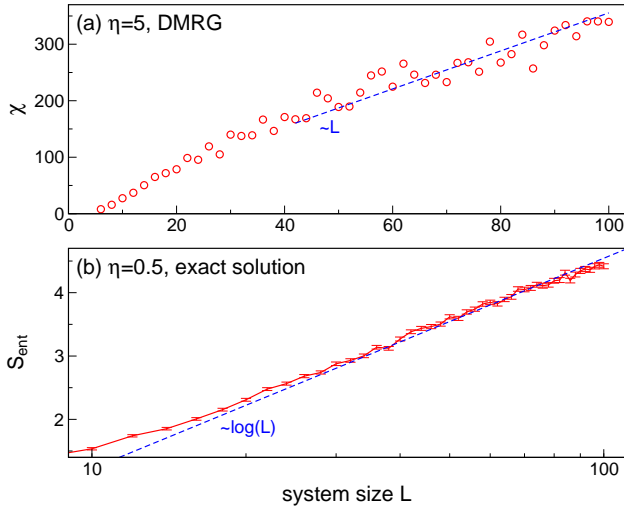
FIG. 8. (Color online) Scaling behavior of an excited state with energy $E/L = -0.125$ in the non-interacting case $\Delta = 0$. (a) DMRG data for the bond dimension at $\eta = 5$. (b) Analytic solution for the entanglement entropy at $\eta = 0.5$. Both support $S(L)/L \sim \log(L)/L$.
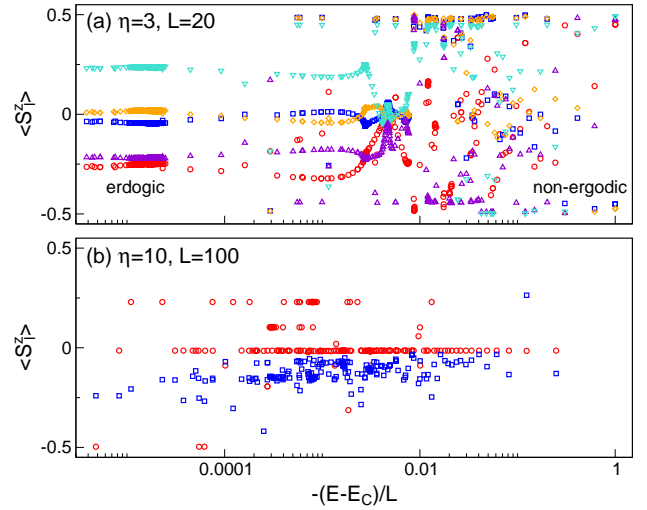

FIG. 9. (Color online) Probing the eigenstate thermalization hypothesis via the expectation value of the local magnetization $\langle S_l^z \rangle$ for $\Delta = 1$ and at various energies. (a) Single configuration drawn at $\eta = 3$ for a chain of $L = 20$ sites (five different positions $l \approx L/2$ are shown). One observes a crossover between thermal and non-ergodic behavior as the energy decreases. (b) Two single configuration drawn at $\eta = 6$ for a large chain with $L = 100$ (only one position $l = L/2$ is shown for each). States at all energies are localized and non-ergodic.

sub-leading logarithmic corrections:

$$\frac{S(L)}{L} \sim \frac{\log(L)}{L}. \tag{10}$$

As the energy increases, we observe a sharp crossover to an exponentially-growing χ (see the inset to Fig. 6) and hence a volume-law scaling of S associated with a metallic phase. Our results are thus consistent with the existence of a mobility edge at $\Delta = 1$ and $\eta = 2.5$ in agreement with the results of Ref. [13]. While in the metallic regime the system sizes that can be tackled by our numerics are similar to those accessible by exact diagonalization, much larger systems can be treated by the excited state DMRG in the localized regime. We elected to study the scaling of the bond dimension instead of calculating the entanglement entropy directly since we observe that the latter exhibits much higher fluctuations and hence requires significantly larger sample sizes to resolve the logarithmic behavior (which is possible but computational even more highly demanding).

Our results for larger disorder are consistent with full many-body localization – states at all energies fulfill an area law with logarithmic corrections up to $L = 100$ sites. This is illustrated in Fig. 7(a) for a large value of $\eta = 5$ lying deep in the MBL phase.

The energy- and interaction-dependence of the entanglement scaling in the localized phase are analyzed more quantitatively in Fig. 7(b) where we fit $\chi = mL$ linearly for $L = 40 \ldots 100$. In the non-interacting case, we find that m is small but finite (this is consistent with the results of Fig. 3). At $\Delta = 0.5$, m increases significantly with increasing energy.

Finally, an important comment is in order: One might wonder whether our result for the scaling of S is an ar-

tifact of the fact that the states computed by our algorithm are potentially a superposition of a large number of nearby eigenstates. For example, the entanglement of an equal superposition of N states is given by $S = \frac{1}{N}\sum_n S^n + \log(N)$, where S^n is the entanglement of each undividual state. Hence, if $N \sim e^L$, this state features a volume law even if an area law holds for each S^n. Even though it is clear that our algorithm does not produce such a specific state (since we do not observe a volume law), it is an obvious question whether our result $S(L) \sim \log(L)$ is a similar artifact. To investigate this, it is instructive to calculate the scaling of S analytically in the non-interacting case. To this end, we determine *pure*, highly-excited eigenstates exactly using the method outlined in Sec. II C and obtain the entanglement entropy using the results of Refs. [42, 43]. Fig. 8 shows that the logarithmic behavior also manifests at $\Delta = 0$ in agreement with our numerics [44]. This strongly suggests that our results are generic.

C. Eigenstate thermalization hypothesis

Another key feature of localized systems is non-ergodic behavior. In a static setup, this can be investigated by checking the eigenstate thermalization hypothesis (ETH), which conjectures that the expectation values of local observables coincide for all states which are close in energy. Fig. 9 displays the energy-dependence of the local magnetization $\langle S_l^z \rangle$ for *single disorder configurations*

(not averages). Energies are shifted with respect to the center of the spectrum of the corresponding individual configuration, which we determine by targeting the highest state of H using conventional ground state DMRG for $-H$.

Fig. 9(a) shows data for $\Delta = 1$ and $\eta = 3$ for a system of size $L = 20$; we expect a coexistence of metallic and localized states. Indeed, the ETH is violated at low energies (large negative E) but holds at high energies. Our DMRG algorithm can now be used to tackle much larger lattices in the MBL phase to demonstrate that states are non-ergodic at all energies. Results are shown in Fig. 9(b) for $L = 100$. As mentioned above, we cannot resolve individual, exponentially close eigenstates but potentially obtain a superposition of nearby states; hence, it was a priori unclear that such a clear violation of the ETH for large many-body localized systems would be observable within our approach.

V. OUTLOOK

We have studied the behavior of excited states in large many-body localized systems using a modified density matrix renormalization group algorithm. The method was benchmarked against exact results constructed in the non-interacting limit. In the MBL phase, the entanglement features an area law with logarithmic corrections. Moreover, our results are consistent with the existence of a mobility edge.

Expressing lowly-entangled excited states of large localized systems in terms of a matrix product state was a long-standing open problem. One can envision a plethora of future applications for the algorithm presented in this work as well as for the closely-related ideas discussed in the preprints of Refs. [34, 35]. Studying the dynamics of perturbations in excited states is one possible avenue.

[1] P. W. Anderson, Phys. Rev. **109**, 1492 (1958).
[2] P. A. Lee and T. V. Ramakrishnan, Rev. Mod. Phys. **57**, 287 (1985).
[3] B. Kramer and A. MacKinnon, Rep. Prog. Phys. **56**, 1469 (1993).
[4] F. Evers and A. D. Mirlin, Rev. Mod. Phys. **80**, 1355 (2008).
[5] D. M. Basko, I. L. Aleiner, and B. L. Altshuler, Ann. Phys. (N.Y.) **321**, 1126 (2006).
[6] R. Nandkishore and D. A. Huse, Annual Review of Condensed Matter Physics, Vol. 6: 15-38 (2015).
[7] V. Oganesyan and D. A. Huse, Phys. Rev. B **75**, 155111 (2007).
[8] M. Žnidarič, T. Prosen, and P. Prelovşek, Phys. Rev. B **77**, 064426 (2008).
[9] C. Monthus and T. Garel, Phys. Rev. B **81**, 134202 (2010).
[10] A. Pal and D. A. Huse, Phys. Rev. B **82**, 174411 (2010).
[11] B. Bauer and C. Nayak, J. Stat. Mech. (2013), P09005.
[12] J. A. Kjäll, J. H. Bardarson, and F. Pollmann, Phys. Rev. Lett. **113**, 107204 (2014).
[13] D. J. Luitz, N. Laflorencie, and F. Alet, Phys. Rev. B **91**, 081103(R) (2015).
[14] R. Vasseur, S. A. Parameswaran, and J. E. Moore, Phys. Rev. B **91**, 140202(R) (2015).
[15] D. A. Huse, R. Nandkishore, V. Oganesyan, A. Pal, and S. L. Sondhi, Phys. Rev. B **88**, 014206 (2013).
[16] A. Chandran, V. Khemani, C. R. Laumann, and S. L. Sondhi, Phys. Rev. B **89**, 144201 (2014).
[17] J. Z. Imbrie, arXiv:1403.7837.
[18] J. H. Bardarson, F. Pollmann, and J. E. Moore, Phys. Rev. Lett. **109**, 017202 (2012).
[19] E. Canovi, D. Rossini, R. Fazio, G. E. Santoro, and A. Silva, Phys. Rev. B **83**, 094431 (2011).
[20] A. Karahalios, A. Metavitsiadis, X. Zotos, A. Gorczyca, and P. Prelovşek, Phys. Rev. B **79**, 024425 (2009).
[21] T. C. Berkelbach and D. R. Reichman, Phys. Rev. B **81**, 224429 (2010).
[22] O. S. Barišić and P. Prelovşek, Phys. Rev. B **82**, 161106(R) (2010).
[23] R. Vosk and E. Altman, Phys. Rev. Lett. **110**, 067204 (2013).
[24] R. Vosk, D. A. Huse, and E. Altman, Phys. Rev. X **5**, 031032 (2015).
[25] S. Gopalakrishnan, M. Müller, V. Khemani, M. Knap, E. Demler, and D. A. Huse, Phys. Rev. B **92**, 104202 (2015).
[26] K. Agarwal, S. Gopalakrishnan, M. Knap, M. Müller, and E. Demler, Phys. Rev. Lett. **114**, 160401 (2015).
[27] Y. Bar Lev, G. Cohen, and D. R. Reichman, Phys. Rev. Lett. **114**, 100601 (2015).
[28] R. Nandkishore, S. Gopalakrishnan, and D. A. Huse, Phys. Rev. B **90**, 064203 (2014).
[29] S. Johri, R. Nandkishore, and R. N. Bhatt, Phys. Rev. Lett. **114**, 117401 (2015).
[30] M. Schreiber et al., Science **349**, 842 (2015).
[31] I. L. Aleiner, B. L. Altshuler, and G. V. Shlyapnikov, Nature Phys. **6**, 900 (2010).
[32] W. de Roeck, F. Huveneers, M. Müller, and M. Schiulaz, arXiv:1506.01505.
[33] M. Friesdorf, A. H. Werner, W. Brown, V. B. Scholz, and J. Eisert, Phys. Rev. Lett. **114**, 170505 (2015).
[34] V. Khemani, F. Pollmann, and S. L. Sondhi, arXiv:1509.00483.
[35] X. Yu, D. Pekker, and B. K. Clark, arXiv:1509.01244.
[36] F. Pollmann, V. Khemani, J. I. Cirac, and S. L. Sondhi,

arXiv:1506.07179.

[37] U. Schollwöck, Ann. Phys. **326**, 96 (2011).

[38] S. R. White, Phys. Rev. Lett. **69**, 2863 (1992).

[39] M. Serbyn, Z. Papić, and D. A. Abanin, Phys. Rev. Lett. **111**, 127201 (2013).

[40] K. Van Acoleyen, M. Mariën, and F. Verstraete, Phys. Rev. Lett. **111**, 170501 (2013).

[41] D. Abanin, W. De Roeck, and F. Huveneers, arXiv:1412.4752.

[42] I. Peschel, J. Phys. A: Math. Gen. **36**, L205 (2003).

[43] J. I. Latorre and A. Riera, J. Phys. A: Math. Theor. **42**, 504002 (2009).

[44] The scaling of the entanglement in the non-interacting limit was also studied in Ref. [45]. For small disorder, the authors observe logarithmic behavior which is a remainder of the area law $S(L) \sim \frac{1}{3} \log(L)$ associated with the clean case. This is *not* the logarithm we observe, which at low energies occurs on a much smaller scale and is not resolved in Ref. [45] where only the ground state is studied.

[45] M. Pouranvari, Y. Zhang, and K. Yang, Advances in Condensed Matter Physics, Volume 2015, Article ID 397630.